Journal of Power Sources 640 (2025) 236700

Contents lists available at ScienceDirect

Journal of Power Sources

journal homepage: www.elsevier.com/locate/jpowsour

# Electrochemical kinetic evolution of electrically neutral redox mediator in electrolyte toward advanced electrochemical energy storage device

Zhenheng Sun [a,b], Min Cao [a,b], Weiwei Gao [a,b,c,*]

[a] Center for Healthcare Materials, Shaoxing Institute, Zhejiang University, Shaoxing, 312099, China
[b] MOE Key Laboratory of Macromolecular Synthesis and Functionalization, Department of Polymer Science and Engineering, Key Laboratory of Adsorption and Separation Materials & Technologies of Zhejiang Province, Zhejiang University, Hangzhou, 310027, China
[c] Shanxi-Zheda Institute of Advanced Materials and Chemical Engineering, Taiyuan, 030032, China

## HIGHLIGHTS

- Analysis of the electrochemical behavior of radicals by a novel MPSM.
- Combined with *in-situ* Raman, an electrochemical kinetic model is developed.
- Concentration polarization-induced radical exchange are critical process.

## ARTICLE INFO

*Keywords:*
Electrochemical energy storage devices
Redox electrolytes
Electrochemical kinetic evolution
Multi-potential steps measurement

## ABSTRACT

As a novel energy storage strategy, redox electrolytes are promising for the high-performance electrochemical energy storage devices with high energy density and power density simultaneously. In comparison to redox mediators in the form of ion-pair reactions, electrically neutral redox mediators with excellent stability exhibit distinctive electrochemical behaviors, which have rarely been systematically explored. In this study, we utilized a typical nitrogen-oxygen radical, 4-hydroxy-2,2,6,6-tetramethyl-piperidinooxy (TEMPO-OH) as an example, combining a novel quasi-steady electrochemical measurement and *in-situ* Raman spectrum to systematically characterize the distribution, diffusion and reaction of radicals during electrochemical processes, finally establish a model for the evolution of electrochemical kinetics. The diffusion of radicals is driven by concentration polarization, whereby a high radical concentration can effectively enhance the capacity and rate performance. Nevertheless, the charge transfer process based on radical exchange and oxidation persists, gradually extending outwards from the electrode/electrolyte interface. As a result, the radical diffusion path is prolonged, and irreversible capacity loss occurs during long-term electrochemical processes, which is detrimental to the enhancement of electrochemical performance. Our research facilitate the development of advanced electrochemical energy storage devices.

## 1. Introduction

The depletion of traditional fossil energy sources and the advent of renewable energy sources strokes highly demands for energy storage solutions [1–3]. Electrochemical energy storage is widely used in daily life as a flexible and efficient energy storage method [4–6]. Traditional electrochemical energy storage devices, such as lithium-ion batteries, supercapacitors, are still limited by the trade-off effect between energy density and power density [7,8]. These results are due to the sluggish diffusion of inert ions within the electrode material, coupled with structural alterations, which inevitably diminish the efficiency of charge transfer. Additionally, the occurrence of electrochemical reactions only at the electrode/electrolyte interface cause the inefficient utilization of the electrode. Notably, the performance of electrochemical energy storage devices depends not only on the electrode materials, but also on the electrolyte [9–11]. The issue can be effectively addressed by the introduction of redox mediators into the electrolyte, which serves to extend the electrochemical reaction from the electrodes to the electrolyte and up to the entire electrochemical energy storage device [12–14]. Moreover, the increasing concentration of redox mediators not only

* Corresponding author. Center for Healthcare Materials, Shaoxing Institute, Zhejiang University, Shaoxing, 312099, China.
*E-mail address:* wwgao@zju.edu.cn (W. Gao).

https://doi.org/10.1016/j.jpowsour.2025.236700
Received 6 January 2025; Received in revised form 14 February 2025; Accepted 1 March 2025
Available online 14 March 2025

improves the efficiency of charge transfer, but also increases the capacity for charge transfer. As a result, electrochemical energy storage devices with excellent electrochemical properties can be achieved.

The typical redox mediators are two transformed ions including $Fe^{2+}/Fe^{3+}$ [15,16], $Fe(CN)_6^{4-}/Fe(CN)_6^{3-}$ [17–19],$V^{2+}/V^{3+}$ [20,21], etc. In spite of ionic couples, there is an electrically neutral redox mediator which has no electrostatic interaction with the electrode at the initial stage of the reaction, exhibiting an excellent stability and low shuttle effect during the electrochemical process. As a typical electrically neutral redox mediator, the nitrogen-oxygen radical, 2,2,6,6-tetramethylperidinooxy (TEMPO) and its derivatives, which have been extensively investigated and applied in supercapacitors and organic redox flow batteries [22–25]. It exhibits ambipolar properties, whereby oxidation occurs at the positive electrode and reduction at the negative electrode during the charging process, thus simplifying the construction of the energy storage system [26–28]. Furthermore, the electron transfer efficiency is considerably higher (in the order of $10^{-2}$ cm $s^{-1}$) than that of other redox mediators [26,29,30], and the reaction potential is approximately 0.8 V vs. SHE [31,32], which allows for the achievement of higher energy and power densities. Nevertheless, related researches mainly focus on the modification of TEMPO and the reaction mechanisms at the interface between electrode and electrolyte [33–35]. The relationship between the electrochemical performance and kinetic mechanism, including the distribution and migration of radicals during the electrochemical process, remains obscure. This presents a significant challenge to the advancement of energy storage systems. Consequently, the utilization of an appropriate characterization method to investigate the kinetic mechanism is of paramount importance.

In this work, we have conducted a comprehensive investigation into the electrically neutral redox electrolyte based electrochemical energy storage devices on the model of a derivative of TEMPO, 4-hydroxy-2,2,6,6-tetramethyl-piperidinooxy (TEMPO-OH). The electrochemical responses of TEMPO-OH at varying concentrations are examined through a quasi-steady electrochemical measurement (i.e., multi-potential steps measurement, MPSM). In combination with the *in-situ* Raman spectrum, the electrochemical kinetics in different potential stages were inferred, allowing for the establishment of a comprehensive electrochemical kinetic evolution. The findings demonstrate that the charge transfer is predominantly influenced by the diffusion rate of TEMPO molecules to the electrode surface, with the procedure primarily governed by the concentration gradient. The impact of the electrostatic interaction can be considered negligible. Furthermore, radical exchange and reaction facilitate the transfer of charge, but this process gradually extends from the electrode surface into the bulk of electrolyte, which is detrimental to electrochemical performance. This work provides an in-depth analysis of the electrochemical behavior of TEMPO radical based electrolytes, and proposes new ideas for the design of advanced electrochemical energy storage devices.

## 2. Experimental section

### 2.1. Pretreatment of the CC electrode

Carbon cloth (CC) sectioned into 1 cm*1.5 cm in size, after being washed several times with ethanol and deionized (DI) water, the CC was dried in a vacuum oven for 6 h. Then, CC was treated in air plasma for 2 min for enhancing its hydrophilicity.

### 2.2. Structural characterization

The morphology of the treated CC was collected on field-emission scanning electron microscopy (FE-SEM, Thermo Scientific Apreo S). Raman spectrum (inVia-Reflex, 532 nm YAG laser) was carried out to examine the changes in the distribution of TEMPO-OH radical at the CC surface during the electrochemical process. The electrolyte diluted to 0.2 mM before and after cycling, was analyzed using a UV–Vis spectrophotometer (Shimadzu UV-1900i).

### 2.3. Electrochemical measurements

The electrochemical behaviors of the CC in TEMPO-OH added electrolyte were performed using a typical three-electrode configuration, with the pretreated CC electrode as the working electrode, a saturated calomel electrode (SCE) and a Pt foil as the reference and the counter electrodes, respectively. The electrolyte was composed of 1 M NaCl and TEMPO-OH with different concentration of 0 mM, 20 mM, 50 mM, 70 mM and 100 mM. Cyclic voltammetry (CV), galvanostatic charge-discharge cycling (GCD) were performed within the potential window of 0–1 V (*vs.* SCE) by using an electrochemical workstation (Chenhua CHI660).

The areal capacity ($Q_A$) of the CC was calculated based on the GCD curves, and the equation is as follows:

$$Q_A = \frac{I\Delta t}{A}$$

Where $I$ is the discharging current, $\Delta t$ is the charging or discharging time, and $A$ is the area of the CC electrode.

To explore the electrochemical kinetics of TEMPO-OH radical with different concentration at the surface of the CC electrode, the multi-potential steps measurement (MPSM) was performed using the same three-electrode configuration. Specifically, a series of potential steps with an increment of 100 mV was applied to the working electrode from 0 V to 1 V (*vs.* SCE). Then, the same potential steps decrement was performed from 1 V to 0 V, each potential stage was maintained for 300 s. Finally, the relationship between the current response and time was analyzed to gain insight into the electrochemical behavior of the redox couple.

## 3. Results and discussion

As a derivative of TEMPO, the solubility of TEMPO-OH in aqueous solutions is significantly enhanced by the introduction of a hydroxyl group, which is of greater utility for energy storage. Furthermore, TEMPO-OH is capable of undergoing oxidation to form $TEMPO\text{-}OH^+$ cations at high potentials and reduction to form $TEMPO\text{-}OH^-$ anions at low potentials, as illustrated in Fig. 1a the introduction of other ions in the electrolyte is necessary to facilitate the transfer between the electrodes during the charge and discharge processes. This enables the balancing of the electrically neutral state, which would otherwise result in an unstable reaction. As shown in Fig. S1, the area of the CV curve demonstrates a progressive increase with the number of cycles. This phenomenon can be attributed to the incomplete reversibility of the reaction, which results in an elevated concentration of $TEMPO\text{-}OH^+$ in the electrolyte and enhanced ionic conductivity, thereby improving the capacitance of the system. Besides, $TEMPO\text{-}OH^-$ is susceptible to attack by protons, which results in the reaction at low potentials being irreversible in a non-alkaline environment [36,37]. As shown in Fig. S2, The oxidation peaks in the CV curves are negligible, and the discharge time in the GCD curves is much shorter than the charging time, corresponding to a very low coulombic efficiency. Consequently, TEMPO-OH is predominantly employed for reactions at the positive electrode with a neutral supporting electrolyte (e.g., NaCl). We have thus investigated the electrochemical behavior at varying concentrations of TEMPO-OH in a 1 M NaCl solution, utilizing hydrophilic-treated carbon cloth (CC) as the electrode. In general, when the concentration is below 10 mM, the capacity contributed by radical species is very limited. Conversely, at concentrations exceeding 100 mM, the system exhibits extremely low coulombic efficiency, rendering both scenarios unsuitable for practical applications. Thus the concentration range is chosen from 10 mM to 100 mM. For convenience in description, we named the systems of CC in 1 M NaCl, 1 M NaCl+10 mM TEMPO-OH, 1 M NaCl+20 mM TEMPO-OH, 1

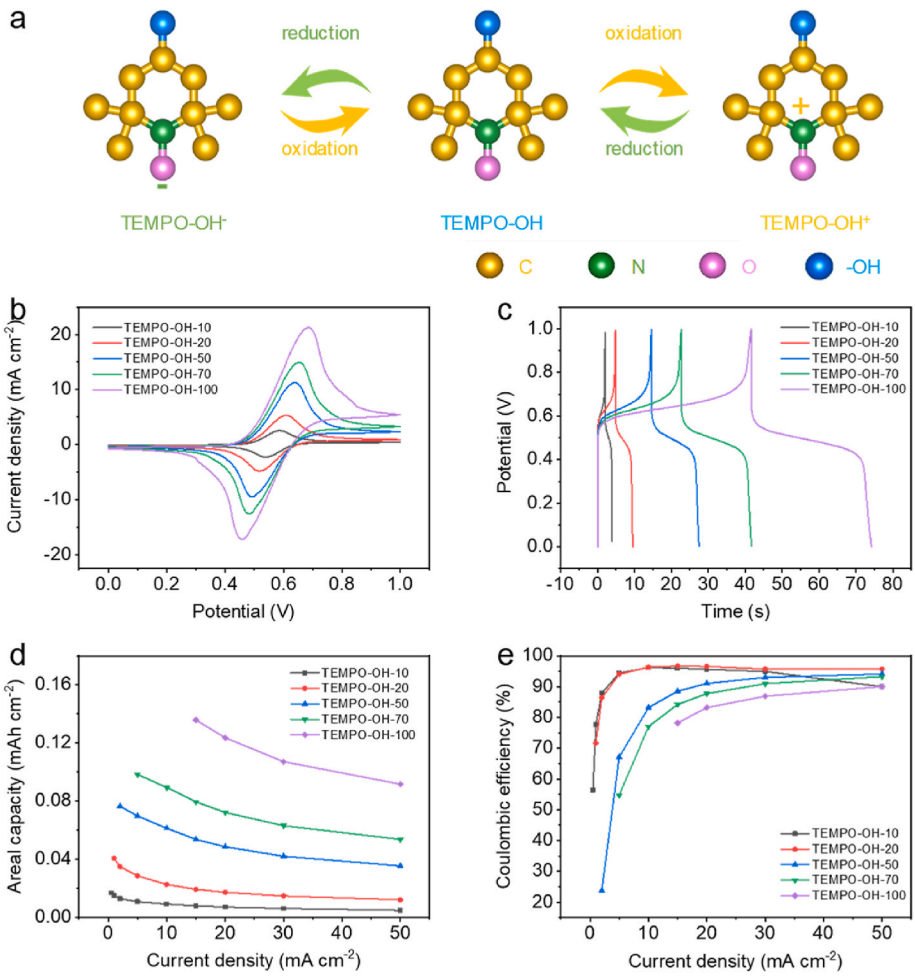


**Fig. 1.** (a) Schematic illustrating the redox reaction of TEMPO-OH; (b) Typical electrochemical performance of carbon-cloth (CC) based electrode in the redox mediators (i.e., TEMPO-OH) added electrolyte with different concentrations: (b) CV curves at 5 mV $s^{-1}$, (c) GCD curves at 15 mA $cm^{-2}$, (d) rate capability derived from the discharging curves at different current densities, and (e) coulombic efficiency at different current densities.

M NaCl+50 mM TEMPO-OH, 1 M NaCl+70 mM TEMPO-OH, and 1 M NaCl+100 mM TEMPO-OH electrolytes as TEMPO-OH-0, TEMPO-OH-10, TEMPO-OH-20, TEMPO-OH-50, TEMPO-OH-70, and TEMPO-OH-100. Fig. S3 illustrates the SEM images of CC, which are composed of carbon fibres with a diameter of approximately 10 μm. This diameter is considerably larger than that of ions and molecules. The surface of CC does not impede the diffusion of ions and molecules, and thus the entire system can be conceptualised as a planar model. The inert electrolyte-based TEMPO-OH-0 exhibits the characteristics of a double electric layer (EDL), as evidenced by a near-rectangular CV curve, a linear GCD curve, and the presence of polarization at high potentials, which can be attributed to the oxygen evolution reaction (Fig. S4).

After introducing TEMPO-OH radicals as redox mediators, the electrochemical behaviors were significantly altered. As illustrated in Fig. 1b, the CV curve of TEMPO-OH-10 exhibits an oxidation peak at 0.58 V and a reduction peak at 0.54 V, resulting in a markedly elevated area compared to that of TEMPO-OH-0. This phenomenon signifies a substantial enhancement in the capacity. Furthermore, the area of the curves demonstrated a continued increase as the concentration of TEMPO-OH increased, indicating that the capacity of the system can be regulated by the concentration of the radical. In addition, the separation between the oxidation and reduction peaks also increases with concentration, indicating that the reaction possesses higher overpotentials. It is inconsistent with the results of GCD (Fig. 1c), which correspond to a faster kinetic process as the separation between the charging and discharging potential platforms decreases with increasing concentration. The discrepancies can be attributed to the fact that the measurement of control voltages is subject to a more pronounced relaxation effect, which will be discussed in more detail below. Furthermore, the current value in the CV curves remains positive at high potentials during the discharge process, indicating that the process cannot be maintained spontaneously. This is consistent with the apparent self-discharge observed in the GCD. Moreover, different systems exhibit a similar potential at the current value of 0, corresponding to the GCD curves in which the IR drop remains constant with an increase in concentration, indicating high stability. The CV curves of different systems with different sweep rates and the GCD with different current densities are presented in Fig. S5, indicating that a faster reaction rate leads to a larger overpotential as well as an IR drop. It is noteworthy that in the GCD test, as the concentration of TEMPO-OH increases, the smaller current densities that cannot be charged to the setting potential. As a consequence, the calculated capacity ranges of different systems based on GCD exhibit a disparity in range of current densities, as illustrated in Fig. 1d. As the concentration of TEMPO-OH increased, the capacity of the systems demonstrated a continuous growth. The corresponding capacity retention at current densities ranging from 15 mA cm-2 to 50 mA cm-2 was calculated to be 61.86 % (TEMPO-OH-10), 62.95 % (TEMPO-OH-20), 66.15 % (TEMPO-OH-50), 67.61 % (TEMPO-OH 70), and 67.53 % (TEMPO-OH-100), demonstrating that an increase in concentration can enhance both capacity and rate performance simultaneously. It is anticipated that this will facilitate the attainment of both elevated energy density and enhanced power density. In addition, it is worth noting

that the rate performance diminishes slightly at high concentrations, implying that there are some factors that can restrict the charge transfer and need to be explored in more depth. Finally, Fig. 1e presents the coulombic efficiencies of the various systems at different current densities. It can be observed that all the systems exhibit low coulombic efficiencies at lower current densities, with efficiency improving as the current density increases. Therefore, within the current density range of 15–50 mA $cm^{-2}$, a concentration of 50–100 mM represents an ideal range that balances high rate performance (>65 %) and coulombic efficiency (>78 %). Notably, the optimal concentration range is significantly influenced by current density. At lower current densities, excessive radical diffusion markedly reduces coulombic efficiency, which becomes more pronounced at higher concentrations. Furthermore, The longer-term charge-discharge cycle data has been provided in Fig. S6. During the initial stages of cycling tests, the incomplete reversibility of the transition from TEMPO-OH to TEMPO-$OH^+$ leads to a decrease in charge capacity and an increase in discharge capacity as the cycle number rises, corresponding to a continuous improvement in coulombic efficiency. Subsequently, the coulombic efficiency stabilizes at ~83 %, indicating that TEMPO-OH is gradually consumed while TEMPO-$OH^+$ diffuses into the bulk of electrolyte. Consequently, the capacity of system gradually decays. After 1000 cycles, the electrolyte transitions from orange to yellow (Fig. S7a), demonstrating the irreversible nature of the reactions. To further characterize changes in the N-O radicals, we analyse the electrolyte before and after cycling using UV–Vis spectrophotometry. As shown in Fig. S7b, the characteristic absorption peak of the radicals in the post-reaction electrolyte exhibits a significant red shift, indicating the conversion of TEMPO-OH to TEMPO-$OH^+$. This transformation is detrimental to the cycling performance of the system. The underlying kinetic mechanism responsible for the observed decline in coulombic efficiency must be subjected to a comprehensive and systematic analysis, employing more appropriate electrochemical measurement techniques.

In order to gain further insight into the electrochemical behavior of radicals, a multi-potential steps measurement (MPSM) was conducted on systems with varying concentrations of TEMPO-OH. Specifically, a series of constant potentials with an interval of 0.1 V were applied within the potential window of 0–1 V, with each potential maintained for 300 s to stabilize the current as much as possible. The kinetic information is then extracted based on the response of the current at different potentials. In the case of TEMPO-OH-0 (Fig. 2a), which represents an inert electrolyte system, a high initial current ($i_i$) is observed at each potential step, returning to zero after an extremely short period of time. The $i_i$ is found to be essentially the same at each potential, which can be regarded as a typical EDL capacitance behavior. In the system containing TEMPO-OH, both the charging and discharging processes can be divided into three distinct stages. Firstly, during the charging process, the current response at low potentials (0–0.4 V) is consistent with that of TEMPO-OH-0, which suggests that a similar EDL capacitance behavior arises from $Cl^-$ adsorption. The initial current at medium potential (0.4–0.7 V) is markedly elevated and requires a longer period of time (steady time, i.e. $t_s$) to reach a steady state, which corresponds to the reaction of free radicals within the EDL. Meanwhile, the final current ($i_f$) is positive and increases with rising concentration of TEMPO-OH. This could provide a rationale for why the redox peak separation in the CV curves increases with increasing concentration. The CV can be regarded as an MPSM with an infinitesimally small step potential and an infinitely brief duration. Consequently, the current is constantly increasing due to the superposition of non-zero $i_f$ of the preceding potential and the current in the moment. It can be observed that as the concentration of TEMPO-OH increases, the value of $i_f$ rises, resulting in a more pronounced superposition effect that leads to a greater separation of the redox peaks. Up to the high potential (0.7–1 V), the $i_i$ reaches a steady state in a very short $t_s$, and the $i_f$ is higher than zero, indicating that the original TEMPO-OH in the EDL has reacted completely. The generated TEMPO-$OH^+$ diffuses to the bulk of the electrolyte, and TEMPO-OH diffuse toward the electrode/electrolyte interface and reacts, such radical exchanges and reactions reach a dynamic equilibrium. Upon switching to a discharge, after the reverse $i_i$ due to EDL reconstruction, the system exhibits a swift transition back to its original positive current. It indicates that the oxidation of TEMPO-OH still dominates. As the potential is further decreased, it takes a longer time for the reverse current to turn into a stable positive current, indicating that there is a competition between TEMPO-OH oxidation and TEMPO-$OH^+$ reduction.

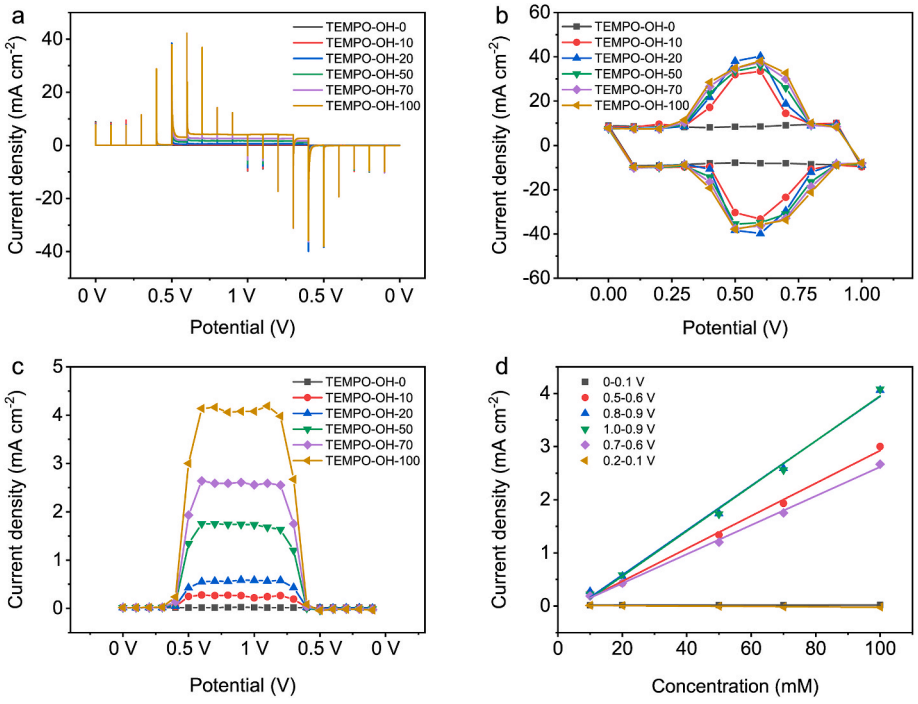


**Fig. 2.** Electrochemical behavior studies of CC in TEMPO-OH added electrolyte with different concentrations: (a) MPSM curves; (b) $i_r$ for different potential stages; (c) $i_f$ for different potential stages; (d) the relationship between $i_f$ and TEMPO-OH concentration.

The latter gradually dominates as the potential decreases until it reaches 0. Finally, at much lower potentials, there is still only a transient reverse current due to the $Na^+$ adsorption.

To further reflect the differences in currents at different concentrations of TEMPO-OH, $i_r$ (i.e., $i_i$-$i_f$) and $i_f$ were extracted, where $i_r$ can be employed to elucidate the rapid response at the electrode/electrolyte interface. To simplify the description, the step from the initial to the termination potential is noted as the initial potential, i.e., the $i_r$ at 0 V represents the current during 0–0.1 V. As evidenced in Fig. 2b, at low potentials, the $i_r$ exhibited a slight decline with increasing TEMPO-OH concentration. This phenomenon may be attributed to the radicals occupying a portion of the adsorption sites on the electrode surface (i.e., steric effect), thereby reducing the amount of $Cl^-$ adsorbed. At medium potentials, the $i_r$ increased markedly with rising TEMPO-OH concentration. This suggests that radicals undergo rapid oxidation, allowing the corresponding reaction currents to be discerned in a brief time span. At high potentials, the $i_r$ is largely similar to that observed at low potentials, indicating that radicals at the interface have undergone complete oxidation, and $Cl^-$ adsorption is the primary process during early stages. During the discharging process, the values of $i_r$ are similar but in opposite directions under most of the potential to that during the charging process. This indicates that the systems exhibit favorable reversibility regardless of radical exchange and reaction. Nevertheless, the $i_f$, as a consequence of radical exchange and reaction, cannot be disregarded. The continuous capacity contribution can have a significant impact on the coulombic efficiency. Fig. 2c illustrates that a large positive current is present throughout the discharging process. Furthermore, the current remains essentially identical within the high-potential range, indicating that the charge transfer in this case is primarily dependent on the concentration of TEMPO-OH. At a certain potential, the reduction of $TEMPO\text{-}OH^+$ is completed rapidly, while the exchange and reaction of TEMPO-OH is highly stable and persists until the potential is altered. Consequently, the longer the duration is conducted, the slower the corresponding electrochemical test process (e.g., low scan rate in CV and small current density in GCD), the more pronounced the oxidation of TEMPO-OH and the lower the corresponding coulombic efficiency. Moreover, at the potential of a reaction, the $i_f$ is linearly correlated with the TEMPO-OH concentration, as illustrated in Fig. 2d. It means that the radical diffusion and reaction based on TEMPO-OH concentration are the rate-determining step (RDS) throughout the entire process. And a larger $i_f$ at high concentration serves to offset the reverse current generated by the reduction of $TEMPO\text{-}OH^+$, corresponding to a lower current density. Therefore, the $i_f$ exerts a significant detrimental impact on the coulombic efficiency of redox electrolyte-based energy storage devices.

To further examine the charge transfer process of radicals, we have analyzed the interrelationship between total charge ($Q_t$) and concentration at various stages, depicted in Fig. 3a. The $Q_t$ is calculated by integrating the MPSM curves at the determinate potentials. At low potentials, the $Q_t$ is so small that it can be considered negligible. It is due to the fact that only the ion adsorption, which is responsible for the formation of the electrical double layer (EDL), contributes to the charge. In the remaining curves, the charge is found to be linearly related to the concentration, thereby confirming that the diffusion of radicals based on concentration polarization represents the RDS for the entire electrochemical process. For the charging process, the maximum growth rate of charge was observed at the medium potential of 0.5–0.6 V. The charge in the process can be divided into two parts based on the following: i) the unsteady charge ($Q_u$), which is contributed by the reaction of TEMPO-OH within the electric double layer (EDL); ii) the drift charge ($Q_d$), which is contributed by the radical exchange and reaction, as illustrated in Fig. S8. In contrast, the total charge in the discharge process was lower at 0.7–0.6 V due to the competition between the reduction of $TEMPO\text{-}OH^+$ as well as the radical exchange and reaction in the process, and the $Q_t$ is calculated by subtracting $Q_u$ from $Q_d$. At the high potentials, the total charge is predominantly derived from the drift charge, as ion adsorption contributes a relatively smaller number of charges. Consequently, the relationship between charge and concentration is essentially identical for both the charging and discharging processes. As previously mentioned, the low coulombic efficiency of the redox electrolyte-based energy storage device is primarily attributable to the $Q_d$ contributed by the stabilised $i_f$. Meanwhile, the charge contributed by the ion adsorption at high and low potentials is insignificant, thereby rendering the $Q_u$ contributed by the radical reaction within the EDL at the medium potential the most favorable for the system. It is noteworthy that the calculated sum of $Q_u$ at the medium potential is nearly identical

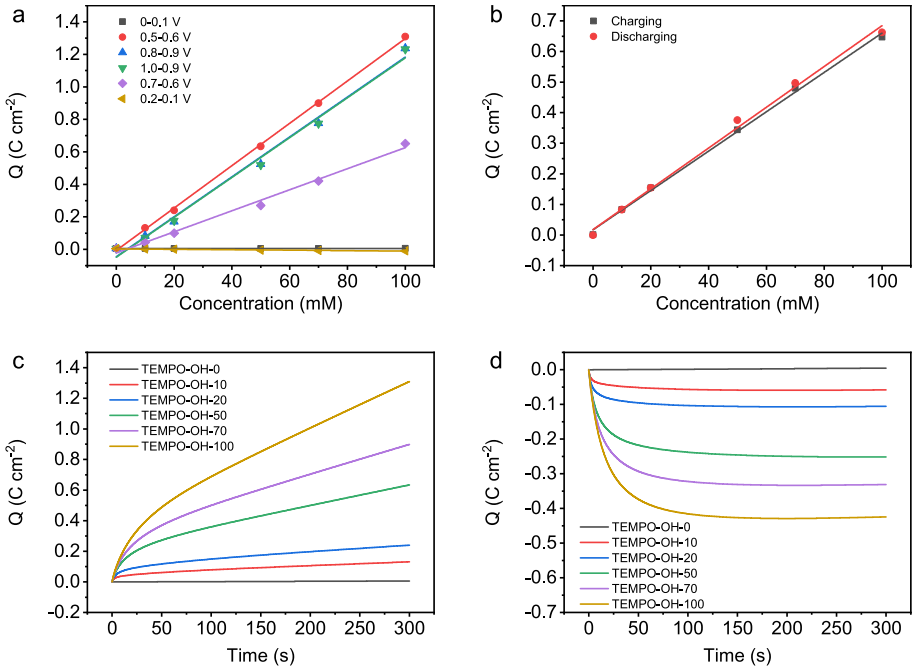


**Fig. 3.** (a) The relationship between $Q_t$ and TEMPO-OH concentration at different potentials; (b) The relationship between the sum of $Q_u$ at 0.4–0.7 V and TEMPO-OH concentration during charging process and discharging process; the relationship between $Q_t$ and time at (c) 0.5–0.6 V and (d) 0.6–0.5 V.

between the charge and discharge processes (Fig. 3b) after subtraction of the $Q_d$, indicating that the reaction within the EDL is totally reversible. It is similarly demonstrated that the drifting charge is disadvantageous for the system, as evidenced not only in the coulombic efficiency but also in the rate performance. Fig. 3c illustrates the relationship between the total charge and time during the charging process within the potential range of 0.5–0.6 V, where the ionic reaction within the bilayer is most significant. In this case, the rate performance can be reflected by the ratio of the total charge at different times. A longer time corresponds to a sluggish electrochemical process. Therefore, the higher the total charge can reach a stable value in a shorter time, the higher the corresponding rate performance. However, due to the contribution of $Q_d$ to the system when the potential is stabilised at 0.6V, which results in an increase in $Q_t$ over time but fails to reach a steady value, it is not possible to achieve a higher rate of performance. While during the discharging process (Fig. 3d), as there is no $Q_d$ present at the potential of 0.5V, the $Q_t$ reaches a stable value after a period of time. Furthermore, the higher the concentration of TEMPO-OH, the higher the growth rate observed in the previous period, which corresponds to a higher rate performance. It can thus be seen that the $Q_d$ generated by radical exchange and reaction in the outer layer of the EDL not only leads to a low coulombic efficiency but also has a detrimental effect on the rate performance. Furthermore, it can be observed that as the concentration of the redox mediators increase, the percentage of $Q_d$ also rises, which in turn restricts the charge transfer at high concentrations, as shown in Fig. 1d. Consequently, a comprehensive examination of the electrochemical behaviour of radicals is essential.

In order to gain insight into the diffusion process of radicals during the electrochemical process, an *in-situ* Raman spectrum was performed in combination with MPSM of CC in 100 mM TEMPO-OH + 1 M NaCl. Specifically, a Raman spectrum of the electrode/electrolyte interface was conducted after the current stabilised at each potential, thus allowing the distribution of radicals as well as the diffusion process at dynamic equilibrium to be analyzed. The measurement potential window was set to 0–0.9 V to prevent the generation of gas bubbles resulting from the oxygen evolution reaction at high potentials, which could potentially impact the accuracy of the detection results. It is noteworthy that no other Raman characteristic peaks for TEMPO-OH are present, with the exception of the hydroxyl group. Consequently, the detection results may be influenced by the hydroxyl characteristic peak of water. Nevertheless, the hydroxyl peak at 3420 $cm^{-1}$ continues to demonstrate a discernible trend during the practical experiment [38,39]. This may be attributed to the pronounced diffusion tendency of a considerable number of radicals within the electric double layer (EDL). As illustrated in Fig. 4, the intensity of the characteristic peak at 3420 $cm^{-1}$ was observed to gradually enhance during the charging process in the low potential range (I), indicating that with the elevation of the potential, the EDL continuously became thicker, and the corresponding radicals migrated to the electrode surface along with $Cl^-$ continuously. As the potential continued to be increased (II), the HTMEPO at the electrode/electrolyte interface underwent a continuous transformation into TEMPO-$OH^+$, which prompted the TEMPO-OH in the electrolyte bulk phase to undergo a continuous diffusion process into the EDL, resulting in a significant enhancement of the corresponding Raman peak signals. Furthermore, there is a sustained increase in the intensity of the associated peak at 3280 $cm^{-1}$, which could be attributed to the continuous production of TEMPO-$OH^+$. This suggests that the vibrational frequency of the hydroxyl group may undergo alteration subsequent to the electron loss. As the potential was further increased (III), the intensity of the corresponding characteristic peaks declined. Meanwhile, the characteristic peaks at lower wave numbers disappeared, suggesting that the TEMPO-$OH^+$ within the EDL is continuously diffusing into the electrolyte bulk phase, and the overall concentration of the radicals was reduced. While in the system switch to discharging process, the intensity of the peaks remains relatively constant in the initial stages, suggesting that only the adsorption of support electrolyte ions can be influenced, rather than the distribution and diffusion of TEMPO-OH. As the potential is reduced to the stage where TEMPO-$OH^+$ can be reduced (IV), the intensity of the characteristic peaks continues to decline, indicating that TEMPO-$OH^+$ continues to diffuse into the bulk of electrolyte after reduction. Finally, as the TEMPO-$OH^+$ within the EDL is depleted, the only remaining capacity in the system comes from that contributed by the EDL. At this point, TEMPO-OH diffuses into the EDL accompanied by $Na^+$ adsorption, corresponding to a recovery of the intensity for the characteristic peaks (V). In consideration of the entirety of the electrochemical process, given that the radicals are electrically neutral, their diffusion driving force is primarily determined by the concentration gradient and the collisions that occur during ion migration.

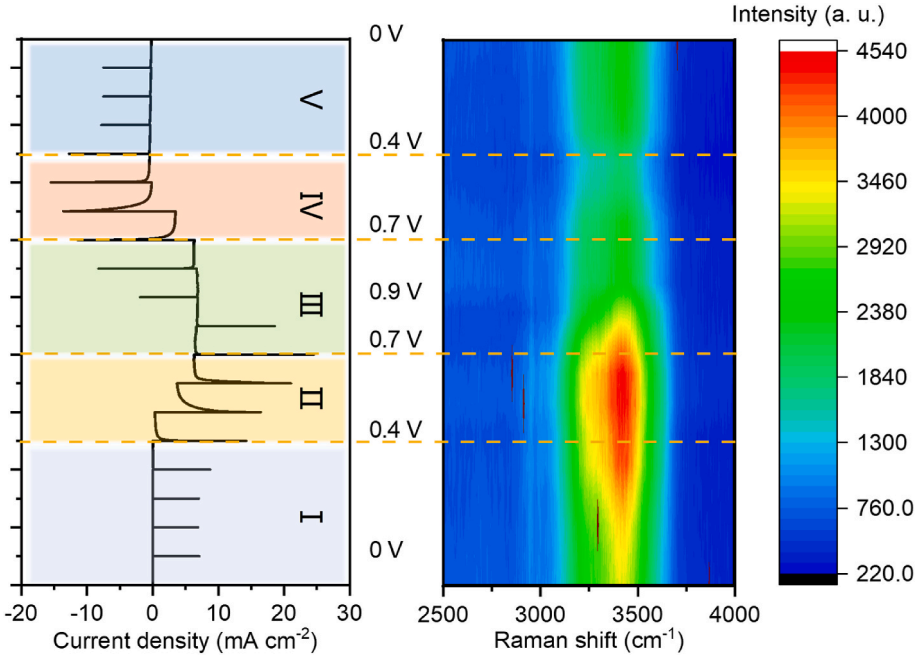


**Fig. 4.** Raman spectra with the corresponding potential based on MPSM with the potential step of 0.1 V and the potential window of 0–0.9 V.

Consequently, the concentration of these radicals exerts a considerable influence on the electrochemical performance.

Based on the characterization and analysis of MPSM as well as the *in-situ* Raman spectrum, an electrochemical kinetic evolution model of the radical redox electrolyte-based energy storage device has been established, as illustrated in Fig. 5. During the charging process, the adsorption of $Cl^-$ initially occurs at low potential as a consequence of the positively charged electrodes, resulting in the formation of the EDL, comprising the Helmholtz layer and the diffusion layer. The Helmholtz layer contains some physically adsorbed radicals, while the diffusion layer consists mainly of $Cl^-$ with some dissociative radicals. As the potential is slightly elevated, the concentration of ions within the EDL is raised and the orientated migration of ions carries more radicals to diffuse into the EDL. As the potential continues to rise, the radicals adsorbed on the electrode surface undergo an oxidation reaction, resulting in the formation of TEMPO-$OH^+$. Subsequently, these species migrate into the diffusion layer under the influence of electrostatic repulsion. While the TEMPO-OH in the diffusion layer migrates to the surface of the electrode and reacts under the driving force from the concentration gradient. The process repeats until the radicals in the EDL are completely reacted out. After that, the radical exchange and reaction will extend from the interior of the EDL to the boundary between the EDL and the bulk of the electrolyte, thereby reaching a dynamic equilibrium, i.e., causing a constant $i_f$. Until higher potentials are reached, the number of adsorbed ions and reacted radicals within the EDL is at equilibrium. Therefore, radical exchange and reaction occur only between the EDL and the bulk of the electrolyte. Upon transitioning to a discharging process, the TEMPO-$OH^+$ is unable to undergo reduction at elevated potentials in a potential-controlled measurement. As a result, radical exchange and oxidation reactions persist following $Cl^-$ desorption and $Na^+$ adsorption, thereby reconstructing the EDL with fewer charge transfer. In contrast, in the current-controlled measurement, the process cannot be maintained spontaneously and the system proceeds directly to the medium potential stage, corresponding to a larger IR drop. At this stage, the reaction of radicals is reversible, with the tendency of the reaction depending on the relative concentration of TEMPO-OH/TEMPO-$OH^+$. As a result of the preceding reaction, the radicals within the EDL are almost totally in the form of TEMPO-$OH^+$. These species are gradually reduced after the attraction of the electrode carrying the negative charge, corresponding to the larger reverse $Q_u$. The reacted radicals diffuse into the bulk of the electrolyte, resulting in a reduction in the concentration of radicals within the EDL. Nevertheless, following a period of reaction, the exchange and oxidation of radicals will occur once more due to the higher concentration of TEMPO-OH in the electrolyte. The process is weakened by a decrease in potential until the TEMPO-$OH^+$ within the EDL is reduced at low potential. Afterward, the migration of TEMPO-OH into the EDL from the bulk of the electrolyte, accompanied by the adsorption of $Na^+$. Therefore, the total concentration of radicals within the EDL is elevated, yet a redox reaction is not feasible. For the whole electrochemical process, the exchange and reaction of radicals between the EDL and the bulk of the electrolyte are primarily dependent on the potential of the system rather than the trend of the potential (i.e., charging or discharging). The continuous process not only reduces the coulombic efficiency by diffusing a portion of TEMPO-$OH^+$ into the bulk of the electrolyte, rendering it unable to transfer charge during discharge, but it also causes the RDS of the entire system to occur in the outer layer of the EDL. This prolongs the diffusion paths of radicals consequently reduces the rate performance. This discovery could even extend to metal batteries [10], offering novel insights for optimizing metal ion deposition/stripping processes in anode systems. Accordingly, for static redox electrolyte-based energy storage devices, the implementation of strategies designed to mitigate this process is of significant importance for the enhancement of performance, including electrode surface modification and the construction of 3D porosity to restrict radical migration.

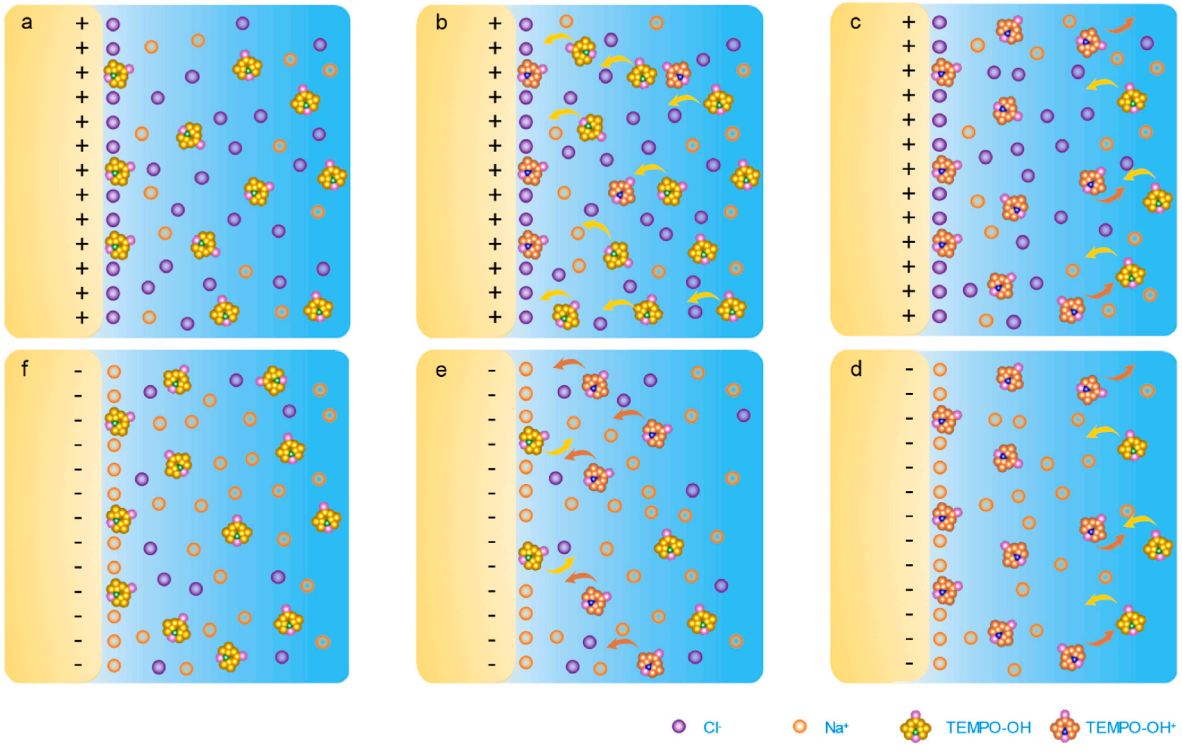


**Fig. 5.** Schematic illustrating the electrochemical behavior of redox electrolyte based on the TEMPO-OH/TEMPO-$OH^+$ couple with CC electrode. (a) low potential, (b) medium potential and (c) high potential stage during charging process; (d) high potential, (e) medium potential and (f) low potential stage during discharging process.

## 4. Conclusions

In conclusion, the comprehensive electrochemical behavior of an electrically neutral redox electrolyte-based electrochemical energy storage device is investigated using a newly developed quasi-steady electrochemical measurement (MPSM) and an *in-situ* Raman spectrum. Consequently, a kinetic evolution model has been formulated to demonstrate that: 1) at the appropriate potential, there is a continuous charge transfer based on the exchange and oxidation of radicals between the EDL and the bulk of the electrolyte. The radical diffusion paths are extended, and a portion of the reacted radicals diffuse into the electrolyte bulk during the process, thereby reducing the coulombic efficiency. 2) As the RDS of the entire process, the radical exchange and oxidation occurring outside the EDL is primarily driven by concentration polarization rather than electrostatic interactions. This process is disadvantageous with regard to the enhancement of energy density and power density, so some strategies are required to mitigate it. Under this guidance, the electrochemical performance of redox electrolyte-based electrochemical energy storage devices can be enhanced with the higher coulombic efficiency. Our work provides a new viewpoint to insight the intrinsic mechanisms underlying the architecture of advanced electrochemical energy storage devices.

## CRediT authorship contribution statement

**Zhenheng Sun:** Writing – review & editing, Writing – original draft, Investigation, Funding acquisition, Conceptualization. **Min Cao:** Writing – review & editing, Investigation. **Weiwei Gao:** Writing – review & editing, Investigation, Funding acquisition.

## Data availability statement

The data that support the findings of this study are available from the corresponding author upon reasonable request.

## Declaration of competing interest

The authors declare that they have no known competing financial interests or personal relationships that could have appeared to influence the work reported in this paper.

## Acknowledgments

We thank Professor Gao Chao from the Department of Polymers at Zhejiang University for his contributions to the mechanism analysis and innovation of the article.

This work is supported by the Natural Science Foundation of Zhejiang Province (No. LR24E030001), Project funded by China Postdoctoral Science Foundation (2023M742973), Shaoxing Technology Projects (NO. 2022B41002), The Joint Research Program of Shaoxing University and Shaoxing Institute, Zhejiang University (2023LHLG008), and the Fundamental Research Funds for the Central Universities (No. 226-2024-00172, No. 226-2024-00074), the Shanxi-Zheda Institute of New Materials and Chemical Engineering (2022SZ-TD011, 2022SZ-TD014).

## Appendix A. Supplementary data

Supplementary data to this article can be found online at https://doi.org/10.1016/j.jpowsour.2025.236700.

## References

[1] G. Kothandam, G. Singh, X. Guan, J.M. Lee, K. Ramadass, S. Joseph, M. Benzigar, A. Karakoti, J. Yi, P. Kumar, Recent advances in carbon-based electrodes for energy storage and conversion, Adv. Sci. 10 (2023) 2301045.

[2] P. Xiong, S. Zhang, R. Wang, L. Zhang, Q. Ma, X. Ren, Y. Gao, Z. Wang, Z. Guo, C. Zhang, Covalent triazine frameworks for advanced energy storage: challenges and new opportunities, Energy Environ. Sci. 16 (2023) 3181–3213.

[3] F. Zhao, B. Wang, W. Zhang, S. Cao, L. Liu, A.Y. Elezzabi, H. Li, W.Y. William, Counterbalancing the interplay between electrochromism and energy storage for efficient electrochromic devices, Mater. Today 66 (2023) 431–447.

[4] C.N. Hong, A.B. Crom, J.I. Feldblyum, M.R. Lukatskaya, Metal-organic frameworks for fast electrochemical energy storage: mechanisms and opportunities, Chem 9 (2023) 798–822.

[5] H. Zhang, Y. Geng, J. Huang, Z. Wang, K. Du, H. Li, Charge and mass transport mechanisms in two-dimensional covalent organic frameworks (2D COFs) for electrochemical energy storage devices, Energy Environ. Sci. 16 (2023) 889–951.

[6] Y. Zheng, N.A. Khan, X. Ni, K.A. Zhang, Y. Shen, N. Huang, X.Y. Kong, L. Ye, Emerging covalent triazine framework-based nanomaterials for electrochemical energy storage and conversion, Chem. Commun. 59 (2023) 6314–6334.

[7] Q. Dou, N. Wu, H. Yuan, K.H. Shin, Y. Tang, D. Mitlin, H.S. Park, Emerging trends in anion storage materials for the capacitive and hybrid energy storage and beyond, Chem. Soc. Rev. 50 (2021) 6734–6789.

[8] R. Zhan, D. Ren, S. Liu, Z. Chen, X. Liu, W. Wang, L. Fu, X. Wang, S. Tu, Y. Ou, A paradigm of calendaring-driven electrode microstructure for balanced battery energy density and power density, Adv. Energy Mater. 13 (2023) 2202544.

[9] Y. Li, X. Zheng, E.Z. Carlson, X. Xiao, X. Chi, Y. Cui, L.C. Greenburg, G. Zhang, E. Zhang, C. Liu, In situ formation of liquid crystal interphase in electrolytes with soft templating effects for aqueous dual-electrode-free batteries, Nat. Energy 9 (2024) 1350–1359.

[10] M. Shen, Z. Dai, L. Fan, H. Fu, Y. Geng, J. Guan, F. Sun, A.M. Rao, J. Zhou, B. Lu, Cosolvent electrolyte chemistries for high-voltage potassium-ion battery, Natl. Sci. Rev. 11 (2024) nwae359.

[11] M. Zheng, T. Liu, J. Wu, X. Tao, Z. Li, S. Zhang, J. Lu, Voltage-induced bromide redox enables capacity restoration of fast-charging batteries, Adv. Mater. (2024) 2414207.

[12] G. Hariharan, S. Arunpandiyan, V. Shanmugapriya, S. Bharathi, M. Babu, B. Selvakumar, A. Arivarasan, Role of various redox additive electrolytes on the electrochemical performances of mixed metal oxide loaded multiwalled carbon nanotube based supercapacitors, J. Energy Storage 57 (2023) 106178.

[13] G. Leverick, Y. Shao-Horn, Controlling electrolyte properties and redox reactions using solvation and implications in battery functions: a Mini-Review, Adv. Energy Mater. 13 (2023) 2204094.

[14] R. Ma, L. Cao, J. Zhuo, J. Lu, J. Chen, J. Huang, G. Yang, F. Yi, Designed redox-electrolyte strategy boosted with electrode engineering for high-performance $Ti_3C_2T_x$ MXene-based supercapacitors, Adv. Energy Mater. 13 (2023) 2301219.

[15] J.P. du Toit, H.M. Krieg, N. Mans, D.J. van der Westhuizen, UV–Vis spectrophotometric analytical technique for monitoring $Fe^{2+}$ in the positive electrolyte of an ICRFB, J. Power Sources 553 (2023) 232178.

[16] M. Nan, M. Wu, Y. Liu, L. Qiao, H. Zhang, X. Ma, Boosting the areal capacity of titanium-manganese single flow battery by $Fe^{2+}/Fe^{3+}$ redox mediator, Small Methods 7 (2023) 2201266.

[17] X. Li, Y. Yao, C. Liu, X. Jia, J. Jian, B. Guo, S. Lu, W. Qin, Q. Wang, X. Wu, Lithium ferrocyanide catholyte for high-energy and low-cost aqueous redox flow batteries, Angew. Chem. Int. Ed. 62 (2023) e202304667.

[18] Z. Chen, T. Li, C. Xie, X. Li, A neutral zinc–iron flow battery with long lifespan and high power density, ACS Energy Lett. 9 (2024) 3426–3432.

[19] H. Zou, Z. Xu, L. Xiong, J. Wang, H. Fu, J. Cao, M. Ding, X. Wang, C. Jia, An alkaline S/Fe redox flow battery endowed with high volumetric-capacity and long cycle-life, J. Power Sources 591 (2024) 233856.

[20] H. Chen, X. Zhang, S. Wu, F. Chen, J. Xu, A comparative study of iron-vanadium and all-vanadium flow battery for large scale energy storage, Chem. Eng. J. 429 (2022) 132403.

[21] Y. Wen, T.P. Neville, A.J. Sobrido, P.R. Shearing, D.J. Brett, R. Jervis, Bismuth concentration influenced competition between electrochemical reactions in the all-vanadium redox flow battery, J. Power Sources 566 (2023) 232861.

[22] L. Hu, L. Xue, J. Fu, P. Xiao, T. Zhai, H. Li, A versatile capacity balancer for asymmetric supercapacitors, Adv. Energy Mater. 10 (2020) 2001608.

[23] X. Yu, W.A. Yu, A. Manthiram, High-energy, single-ion-mediated nonaqueous zinc-TEMPO redox flow battery, ACS Appl. Mater. Interfaces 12 (2020) 48654–48661.

[24] B. Hu, M. Hu, J. Luo, T.L. Liu, A stable, low permeable TEMPO catholyte for aqueous total organic redox flow batteries, Adv. Energy Mater. 12 (2022) 2102577.

[25] E. Pedraza, C. de la Cruz, A. Mavrandonakis, E. Ventosa, R. Rubio-Presa, R. Sanz, S. T. Senthilkumar, P. Navalpotro, R. Marcilla, Unprecedented aqueous solubility of TEMPO and its application as high capacity catholyte for aqueous organic redox flow batteries, Adv. Energy Mater. 13 (2023) 2301929.

[26] L. Hu, C. Shi, K. Guo, T. Zhai, H. Li, Y. Wang, Electrochemical double-layer capacitor energized by adding an ambipolar organic redox radical into the electrolyte, Angew. Chem. 130 (2018) 8346–8350.

[27] K. Hatakeyama-Sato, K. Oyaizu, Redox: organic robust radicals and their polymers for energy conversion/storage devices, Chem. Rev. 123 (2023) 11336–11391.

[28] Q. Hu, S. Cui, K. Sun, X. Shi, W. Miao, X. Wang, H. Peng, G. Ma, A redox-active dual-network hydrogel electrolyte for flexible supercapacitor, J. Energy Storage 68 (2023) 107815.

[29] K. Zhang, Y. Hu, L. Wang, M.J. Monteiro, Z. Jia, Pyrene-functionalized PTMA by NRC for greater π–π stacking with rGO and enhanced electrochemical properties, ACS Appl. Mater. Interfaces 9 (2017) 34900–34908.

[30] B. Chen, Z. Lu, S. Feng, Z. Zhou, C. Lu, Redox-active nitroxide radicals grafted onto MXene: boosting energy storage via improved charge transfer and surface capacitance, ACS Energy Lett. 8 (2023) 1096–1106.

[31] O. Nolte, P. Rohland, N. Ueberschaar, M.D. Hager, U.S. Schubert, Stability of TMA-TEMPO-based aqueous electrolytes for redox-flow batteries, J. Power Sources 525 (2022) 230996.
[32] X.-L. Lv, P.T. Sullivan, W. Li, H.-C. Fu, R. Jacobs, C.-J. Chen, D. Morgan, S. Jin, D. Feng, Modular dimerization of organic radicals for stable and dense flow battery catholyte, Nat. Energy 8 (2023) 1109–1118.
[33] S. Mitra, A. Heuer, D. Diddens, Electron transfer reaction of TEMPO-based organic radical batteries in different solvent environments: comparing quantum and classical approaches, Phys. Chem. Chem. Phys. 26 (2024) 3020–3028.
[34] J.E. Nutting, M. Rafiee, S.S. Stahl, Tetramethylpiperidine N-oxyl (TEMPO), phthalimide N-oxyl (PINO), and related N-oxyl species: electrochemical properties and their use in electrocatalytic reactions, Chem. Rev. 118 (2018) 4834–4885.
[35] T. Suga, Y.-J. Pu, K. Oyaizu, H. Nishide, Electron-transfer kinetics of nitroxide radicals as an electrode-active material, Bull. Chem. Soc. Jpn. 77 (2004) 2203–2204.
[36] X. Wei, W. Pan, W. Duan, A. Hollas, Z. Yang, B. Li, Z. Nie, J. Liu, D. Reed, W. Wang, Materials and systems for organic redox flow batteries: status and challenges, ACS Energy Lett. 2 (2017) 2187–2204.
[37] H. Fan, B. Hu, H. Li, M. Ravivarma, Y. Feng, J. Song, Conjugate-driven electron density delocalization of piperidine nitroxyl radical for stable aqueous zinc hybrid flow batteries, Angew. Chem. Int. Ed. 61 (2022) e202115908.
[38] H. Jin, J. Zhou, J. Tao, Y. Gu, E. Kan, Z. Yao, B. Ouyang, Dielectric loss compensation induced by hydroxyl surface grafting protects against microwave absorption attenuation, Carbon 216 (2024) 118571.
[39] S. Mohammadi, A.M. Homayounfard, S.M. Mousavi–Khoshdel, Experimental and theoretical investigation of high-performance supercapacitor based on guanidine functionalized graphene oxide, Electrochem. Commun. 163 (2024) 107703.